

M. Brombin, A. Boboc, A. Murari, E. Zilli, L. Giudicotti
and JET EFDA contributors

Systematic Comparison between Line Integrated Densities Measured with Interferometry and Polarimetry at JET

“This document is intended for publication in the open literature. It is made available on the understanding that it may not be further circulated and extracts or references may not be published prior to publication of the original when applicable, or without the consent of the Publications Officer, EFDA, Culham Science Centre, Abingdon, Oxon, OX14 3DB, UK.”

“Enquiries about Copyright and reproduction should be addressed to the Publications Officer, EFDA, Culham Science Centre, Abingdon, Oxon, OX14 3DB, UK.”

Systematic Comparison between Line Integrated Densities Measured with Interferometry and Polarimetry at JET

M. Brombin^{1,2}, A. Boboc³, A. Murari¹, E. Zilli^{1,2}, L. Giudicotti^{1,2}
and JET EFDA contributors*

JET-EFDA, Culham Science Centre, OX14 3DB, Abingdon, UK

¹*Consorzio RFX, Associazione EURATOM-Enea sulla fusione, Corso Stati Uniti 4, I-35127, Padova Italy*

²*Electrical Engineering Department, Padova University, via Gradenigo 6-A, 35131 Padova, Italy*

³*EURATOM-UKAEA Fusion Association, Culham Science Centre, OX14 3DB, Abingdon, OXON, UK*

** See annex of M.L. Watkins et al, "Overview of JET Results ",
(Proc. 21st IAEA Fusion Energy Conference, Chengdu, China (2006)).*

ABSTRACT

A systematic comparison between the line integrated electron density derived from interferometry and polarimetry at JET has been carried out. For the first time the reliability of the measurements of the Cotton-Mouton effect has been analysed for a wide range of main plasma parameters and the possibility to evaluate the electron density directly from polarimetric data has been studied. The purpose of this work is to recover the interferometric data with the density derived from measured Cotton-Mouton effect, when fringe jump phenomena occur. The results show that the difference between the line integrated electron density from interferometry and polarimetry is with one fringe ($1.143 \times 10^{19} \text{ m}^{-2}$) for more than 90% of the cases. It is possible to consider polarimetry as a satisfactory alternative method to interferometry to measure the electron density and it could be used to recover interferometric signal when a fringe jumps occurs, preventing difficulties for the real-time control of many experiments at the JET machine.

1. INTRODUCTION

Real-time electron density profile measurements are essential for advanced fusion tokamak operation and multichannel infrared interferometry is a proven method for measuring density. Nevertheless, interferometric method can be affected by some problems. In particular, in the JET machine, the far infrared (FIR) interferometer ($\lambda = 195 \mu\text{m}$) [1] is subject to occasional fringe jumps, as a consequence of events such as Edge Localised Modes (ELMs) [2], fast density increases, disruptions [3] and pellet injection. Due to these effects, the interferometric signal can be corrupted or even lost for significant intervals of time, resulting in an unreliable reconstruction of the measured phase angle. This phenomenon prevents the use of the measured line integrated density in a real-time feedback controller. To solve this problem alternative methods for measurements of density have been considered as, for example, the polarimetry based on the Cotton-Mouton effect [4],[5],[6]. Far infrared multichannel polarimetry has been traditionally employed in toroidal machines to evaluate the poloidal magnetic field profile using the Faraday effect. From the measurement of the Faraday rotation angle and using the electron density provided by interferometry, the plasma current density profile and the safety factor q can be derived directly [7]. In tokamaks, due to the toroidal magnetic field perpendicular to the propagation direction of the probing beam, an effect on ellipticity of beam polarization is also observed. It is the so called Cotton-Mouton effect and it has been widely studied [8][9]. Since in tokamak the toroidal field is known, this effect gives the possibility of obtaining the line integrated electron density from the measurement of the ellipticity of the probing beam. The use of the Cotton-Mouton effect for the measurement of the line integrated density has been experimentally demonstrated in the W7-AS stellarator, where the measurements have been compared with the interferometric ones [10].

For these reasons, also in the JET machine, the possibility of obtaining the electron density from measurements of the Cotton-Mouton effect has been seriously considered and to this purpose the existing FIR interferometer/polarimeter system has been upgraded [4].

At JET, in the last years the Cotton-Mouton effect and the measurement of line integrated electron density from polarimetric data have been theoretically studied and experimentally characterized. These studies include the separation of the Faraday and the Cotton-Mouton effects when they do not combine linearly [11], the statistical comparisons of electron density measurements from polarimetry with the same data from interferometry [4][12] and a comparison of the experimental polarimetric data with those evaluated by a numerical solution of the polarization evolution equation and by some approximate analytical solutions [6].

The present work reports a new systematic comparison of the line integrated electron density derived from interferometry and from polarimetry at JET, over an extended range of the main plasma parameters, in particular for high values of electron density. The polarimetric data has been processed by means of a simple approximation of the evolution equation considering small plasma effects. The adopted approximation seems to provide better results than the one adopted in a previous work [12]. The main purpose consists of recovering interferometric data, when they are affected by fringe jumps, with the density obtained by the measured Cotton-Mouton effect. A systematic analysis of the reliability of the Cotton-Mouton measurements for a wide range of plasma conditions in JET (different regimes of temperature, density and toroidal magnetic field) is presented for the first time. The method used in this work to process the polarimetric signals has been verified comparing the results with those provided by a numerical wave propagation code which evaluates the output polarization, taking into account data from Thomson Scattering, magnetic probes and an equilibrium code (EFIT).

This method to measure the line integrated density, alternative to interferometry, could be widely employed in the future large fusion machines, i.e. ITER [14].

2. POLARISED WAVES IN MAGNETISED PLASMAS

The polarization state of an electromagnetic wave can be described by the reduced Stokes vector $s \equiv (s_1, s_2, s_3)$ [15]

$$s_1 = \cos 2\chi \cos 2\psi = \cos 2\Theta \quad (1)$$

$$s_2 = \cos 2\chi \sin 2\psi = \sin 2\Theta \cos 2\Phi \quad (2)$$

$$s_3 = \sin 2\chi = \sin 2\Theta \sin \Phi \quad (3)$$

where s_i ($i = 1, 2, 3$) can be expressed as a function of geometric parameters ψ and χ (the polarization angle and the ellipticity $\epsilon = \tan\chi$) or of the amplitude ratio $\tan\Theta$ and the mutual phase shift angle Φ of the two sinusoidal components (E_x and E_y) of the electric field vector E (see Figure 1). The evolution of the polarization is described, as a function of the propagation direction z , by the vector equation

$$\frac{ds(z)}{dz} = \Omega(z) \times s(z) \quad (4)$$

where the components of vector Ω , in the case of cold plasma and $\dots \omega_p^2 \ll \omega^2$, $\omega_c \ll \omega$, (ω_p , ω_c and ω being the plasma, electron cyclotron and probing wave frequency respectively), depend on plasma density and magnetic field B [17]

$$\begin{pmatrix} \Omega_1 \\ \Omega_2 \\ \Omega_3 \end{pmatrix} = \frac{\omega_p^2}{2c\omega^3} \times \begin{pmatrix} \frac{e^2}{m_e^2} (B_x^2 - B_y^2) \\ 2 \frac{e^2}{m_e^2} B_x B_y \\ 2 \frac{e}{m_e} \omega B_z \end{pmatrix} \quad (5)$$

with $\omega_p^2 = n_e e^2 / m_e \epsilon_0$ and B_x , B_y and B_z are the perpendicular, radial and the parallel components of the magnetic field with respect to the wave's propagation direction, as shown in Figure 6. The magnetic field has two effects on the state of output polarization: the changes in the ψ angle, or rotation of the major axis of the polarization ellipse, and the changes in the x angle, or in the ellipticity. The rotation of the plane of polarization is mainly related to the Faraday effect. The change in the ellipticity is mainly related to the Cotton-Mouton effect, that arises from the magnetic field perpendicular to the direction of propagation. It is useful to define the quantities:

$$W_i \equiv \int_{z_1}^{z_2} \Omega_i(z) dz \quad \text{where } i = 1, 2, 3 \quad (6)$$

where z_1 and z_2 are the extremes of the path of the polarization beam inside the vessel. In a tokamak with $B_x^2 B_y^2$ and for vertical chords (toroidal magnetic field $B_t = B_x = \text{const.}$) W_1 can be approximated as:

$$W_1 = C_1 \lambda^3 B_t^2 \int_{z_1}^{z_2} n_e(z) dz, \quad (7)$$

with $C_1 = e^4 / (16\pi^3 c^4 m_e^3 \epsilon_0) = 2.44 \times 10^{-11} \left[\frac{\text{rad}}{\text{m T}^2} \right]$. If W_1 is known, the line integral of the electron density is given by:

$$\int_{z_1}^{z_2} n_e(z) dz = \frac{W_1}{C_1 \lambda^3 B_t^2} \quad (8)$$

This possibility represents an interesting alternative method to traditional interferometry.

3. THE INTERFEROMETER/POLARIMETER DIAGNOSTIC AT JET

At JET, the Far Infrared (FIR) diagnostic operates as a dual interferometer/polarimeter system, widely described in [1]. Among all the elements of this diagnostic set-up it should be mentioned that the radiation source is a DCN laser at $\lambda = 195\mu\text{m}$ and the reference beam is modulated at a frequency ω_0 (100 kHz) by means of a rotating grating. The system probes the plasma with 4 vertical and 4 lateral (see Figure 6) laser beams which provide line-integrated measurements of the plasma density and Faraday angles by means of interferometry and polarimetry respectively. After an optimization of the hardware and implementation of a new set-up for this diagnostic, it is now possible to measure routinely the Faraday rotation angle and the Cotton-Mouton effect simultaneously on two vertical channels [4]. The interferometer measurements are integrated into the real-time control of plasma, and are used for machine protection against disruptions.

3.1. THE INTERFEROMETER: PRINCIPLE

In the context of Magnetic Confinement Fusion (MCF) experiments, this instrument normally consists of a laser beam, which is splitted into several separate beams, one of which does not interact with the plasma and is used as reference. The others traverse the plasma and therefore their phase is affected by the properties of the plasma. The difference in phase is given by

$$\Delta\phi = \frac{\omega}{2cn_c} \int_{z_1}^{z_2} n_e(z) dz \quad (9)$$

where $n_c = \omega^2 m_e \epsilon_0 / e^2$ is the critical density.

For the experimental set up the measured $\Delta\phi_0$ is in the $[-\pi, +\pi]$ range but the true value of $\Delta\phi$ can be higher than 2π :

$$\Delta\phi = \Delta\phi_0 + 2\pi F, \quad (10)$$

where F is an integer representing the fringe number. When, for example, a rapid phase variation larger than 2π or, as well, a temporary deflection of the measuring beam occurs, the fringe number cannot be determined then measurement fails. Such events are usually called fringe jumps and they introduce discontinuities on the phase evaluation equal to an integer number of multiples of 2π . In the case of JET, the main phenomena which may cause fringe jumps are typically ELMs and pellets. In the case of ELMs, one or more beams passing through the plasma can be diffracted away from the detector. In experiments with pellet injection the acquisition sampling rate sometimes is not high enough to track the fast changes of the plasma density occurring between two subsequent samples. The corresponding error in the line density may be large; in particular for the JET interferometer a fringe jump on phase measurement introduces a line density error equal to $9.8 \times 10^{18} \text{ m}^{-2}$

3.2. THE POLARIMETER

The classical application of polarimetry is the measurement of the Faraday rotation angle for a set of beams propagating through the plasma. The poloidal magnetic field profile is determined by inversion methods [7] and from this the plasma current density and the profile of the safety factor q can be derived. This is very simple when $\Omega_3 \gg \Omega_1, \Omega_2$, (dominant Faraday effect) because the observed polarization rotation gives directly the Faraday rotation angle. In tokamaks, where the toroidal field B_t is higher than the poloidal one, the parameters Ω_1 can be not negligible with respect to Ω_3 and the change in the ellipticity can be significant (Cotton-Mouton effect). In JET, the Faraday rotation angle is measured on all 8 channels by evaluating two perpendicular polarization components of the laser beam probing the plasma. The measurement of the Cotton- Mouton effect, has been implemented only on the vertical chords, where the linear polarization of the input beam is set at 45° with respect to the toroidal field direction.

A half-wave plate at the entrance window is used to set the required direction of the linear input polarization and can be rotated to provide an on-line calibration before each discharge. After traversing the plasma, a linear polarized beam suffers a rotation of the polarization plane due to Faraday rotation and acquires ellipticity due to the Cotton-Mouton effect. As described in [1], the beam resulting from the recombination between the probing and the reference beams is splitted by a wire grid along the x and y directions and focused onto two detectors ('interferometer detector' and 'polarimeter detector' respectively). The two detectors give beat signals at the frequency ω_0 :

$$i(t) = A_1 \cos \omega_0 t \quad (11)$$

$$p(t) = A_p \cos(\omega_0 t - \varphi). \quad (12)$$

They are electronically processed as described in [4] to obtain, with the aid of a calibration, the two angles Θ and Φ of the probing beam outgoing from the plasma. From these data, the other polarization parameters can be evaluated using the relations (1, 2, 3).

4. MODELLING OF THE MEASUREMENTS AND NUMERICAL VALIDATION

As previously introduced, this work aims to test the reliability of the line integrated plasma density obtained from polarimetric data. In general the exact solution of evolution equation (4) shows a mutual interference between the Faraday effect and the Cotton-Mouton effect, such that it may be difficult to separate them [9]. To our purpose, it is convenient to consider the following approximate solution [16]:

$$s(z) \cong s_0 + s_0 \times \int_{z_1}^{z_2} \Omega(z) dz \quad (13)$$

where s_0 is the initial polarization state and it is valid in the condition

$$W(z) \ll 1, \quad (14)$$

with

$$W(z) \equiv \int_{z_1}^{z_2} |\Omega(z')| dz'. \quad (15)$$

The previous condition is equivalent to assuming that the effect of the plasma on the polarization state of the beam is small. In this approximation it is possible to evaluate the final polarization state from the initial condition. The result can be put in the form:

$$s_f = M \cdot s_0 \quad (16)$$

where M , the transition matrix of the plasma [17], is given by:

$$M \equiv \begin{pmatrix} 1 & -W_3 & W_2 \\ W_3 & 1 & -W_1 \\ -W_2 & W_1 & 1 \end{pmatrix} \quad (17)$$

For a generic input polarization s_0 , the rotation of the polarization depends not only on W_3 , but also on W_1 and W_2 , and the ellipticity depends on W_1 and also on W_2 . For input beam linearly polarized at 45° , whose Stokes vector is $s_0 = (0, 1, 0)$, the final Stokes vector can be written as:

$$s_f \approx (-W_3, 1, W_1), \quad (18)$$

which, for $|W_1| \ll 1$ and $|W_3| \ll 1$, represents a polarization rotated by an angle $\psi \approx W_3/2$ with respect to the initial 45° (Faraday effect) and with an ellipticity $\hat{I} \approx W_1/2$ (Cotton-Mouton effect associated with the 1 component)[9]. This result is particularly interesting because the two effects satisfy the relations for the Faraday effect and the Cotton-Mouton effect respectively, without any interference. Then it is possible to link the line integrated plasma density directly to the ellipticity of the polarization using the following equations:

$$s_{3f} = \sin 2\chi \quad (19)$$

$$s_{3f} \approx W_1. \quad (20)$$

The former is the definition for the third Stokes vector component and the latter is a consequence of the present approximation. Using equation (8) it is possible to write:

$$n_e(z)dz = \int_{z_1}^{z_2} \frac{\sin 2\chi}{C_1 \lambda^3 B_t^2} dz \quad (21)$$

From the ellipticity measured by the polarimeter it is possible to reconstruct the line integrated plasma density with good agreement with interferometry. Figure 4 shows, as an example, the time evolution of the line integrated electron density measured by interferometry together with the one measured by polarimetry using relation (21). The agreement between the two curves demonstrates the capability of the polarimeter to provide a reliable measurement of the line integrated density. This measurement can also be performed using parameters Θ and Φ related to the polarization ellipse (Figure 1). Indeed the s_{3f} component can be expressed as a function of Θ and Φ according to (3) and so:

$$\int_{z_1}^{z_2} n_e(z)dz = \frac{\sin 2\Theta \sin \Phi}{C_1 \lambda^3 B_t^2} \quad (22)$$

It is interesting to compare equation (22) with an analogue equation proposed in [12], [5] where the phase shift Φ is used:

$$\int_{z_1}^{z_2} n_e(z)dz = \frac{\Phi}{C_1 \lambda^3 B_t^2} \quad (23)$$

As can be seen, equation (22) is more general than (23), they are equal when the phase shift is small ($\sin \Phi \approx \Phi$) and the angle remains constant at 45° . At JET, it has been experimentally observed that these conditions are not always satisfied, so it is more appropriate to use equation (21), which relies on only one polarimetric parameter, for determining the line integrated density, instead of (22) which requires the measurement of two parameters.

5. COMPARISON OF THE ELECTRON DENSITY OBTAINED WITH THE POLARIMETER AND THE INTERFEROMETER

A large number of JET pulses covering different plasma conditions have been investigated. The selected shots belong to various campaigns (years 2006 and 2007), to produce statistics without any particular bias linked to particular experiments. The considered plasma parameters are the toroidal magnetic field, the electron temperature, the total additional power (NBI+ICRH+LHCD) and the plasma current. For each shot, the representative points of these parameters, covering a large number of plasma scenarios, are shown in Figure 5 as a function of the interferometric line integrated density in the range between 0 and $3 \times 10^{20} \text{ m}^{-2}$. As it can be noticed the toroidal magnetic field is up to 3.5T, the electron temperature up to 10keV, the additional power up to 30MW and the plasma current up to 3.5MA. The values of Faraday rotation angle and ellipticity, coming from polarimetric measurements, are also plotted in the same figure. It is interesting to underline the linear dependence between these two last parameters and the density from interferometry.

Faraday rotation angles greater than 15% are not shown here because of the limitations imposed by the actual set-up for calibration.

The two parameters W_1 and W_3 , represented in Figure 6, have been calculated as integrals of $\Omega_1(z)$ and $\Omega_3(z)$, taking into account the density profiles and the magnetic field configurations; the former are provided by Thomson Scattering and the latter by the MHD equilibrium code used at JET. It is clear that the two parameters are less than 0.2 radians and in most of the cases their values are less than 0.1 radians. The quantity $W(z)$, defined in (15) may be expected to be of the same order of magnitude. This only fact isn't enough to consider correct the approximate solution (13) of the evolution equation, with the consequences exposed in section 4. Nevertheless a confirmation of the reliability of the approximation (13) comes from the comparison between s_{3f} and $\sin 2\chi$, as suggested by equation (19); the former is obtained as numerical solution of the evolution equation (4) with the profiles of $\Omega_1(z)$ and $\Omega_3(z)$, given by other diagnostics, and the latter is deduced by polarimetric measurements. As shown in Figure 7 the estimated value of s_{3f} agrees with the experimental measurement of $\sin 2\chi$ within a maximum error of $\pm 5\%$. Given this agreement between polarimetric measurements and data from other diagnostics, it is possible to supposed correct the approximation adopted here.

After this, the line integrated plasma density has been evaluated using the polarimetric data and compared with the one from interferometry. Figure 8 shows the difference between the density obtained by polarimetric data and the density from the interferometer expressed in terms of fringes (one fringe = $1.143 \times 10^{19} \text{ m}^{-2}$) as a function of the line integrated electron density from interferometer; in this way it is easy to find when the agreement is within one fringe, which represents the interferometric error. In particular, in Figure 8a, the density evaluated by equation (23), using the phase shift $\Delta\phi$, is compared with the density from interferometry. The agreement is within one fringe just for densities less than $12 \times 10^{19} \text{ m}^{-2}$. On the other hand, in Figure 8b, where the density evaluated using equation (21) is compared to the interferometric density, it can be easily noticed that the agreement is within one fringe for all the density range considered. In particular for high electron line density values all points plotted are within the dotted red-line representing the threshold of plus/minus one fringe.

The results of Figure 8 are better presented from a quantitative point of view in Figure 9. The bars of histograms represent the fraction of points (in percents) for which the difference between density from polarimetry and from interferometry is within a fringe ($1.143 \times 10^{19} \text{ m}^{-2}$) over three different density ranges ($0 - 10 \times 10^{19}$, $10 - 20 \times 10^{19}$, $20 - 30 \times 10^{19}$) and three time ranges (40-47s, 47-60s and 60-70s). The considered time ranges correspond to ramp up, steady state and ramp down plasma phases respectively. The bars marked as PHS and as EXP correspond to data obtained using relations (23) and (21) respectively. It is clear that using equation (23) the agreement is within one fringe for densities up to $15 \times 10^{19} \text{ m}^{-2}$, but for higher densities is absent (about 1%), with a difference of about five fringes. Using relation (21), the agreement is within one fringe in more than 90% of the cases, so that it is satisfactory for the entire range of densities, and it is very good (99%) for densities higher than $20 \times 10^{19} \text{ m}^{-2}$.

SUMMARY

A comparison between density from interferometry and from polarimetry has been presented for the first time considering many JET pulses. A method to measure the line integrated electron plasma density alternative to interferometry is needed to provide informations on density when the interferometric signal is affected by fringe jumps. In this case, the idea is to provide to interferometer the correct value of density, so its signal can be recover.

Looking at the results reached with this work it is possible to conclude that polarimetry could be used to recover interferometric signal when a fringe jump occurs, which otherwise could result in serious difficulties for the plant safety and real-time control of many JET experiments [19]. When both the Faraday and Cotton-Mouton effects are small enough ($|W_3|, |W_1| < 0.2$), using a simple solution of the evolution equation (4), the density can be evaluated from polarimetric data. Finally, this type of analysis is going to be performed for channels 2 and 4 at JET and these results will contribute and support the design of ITER interferometer/polarimeter.

ACKNOWLEDGEMENTS

The authors would like to thank O. Ford, L. Zabeo and F. Orsitto for their useful and interesting suggestions. This work, supported by the European Communities under the contract of Association between EURATOM and ENEA, was carried out within the framework of European Fusion Development Agreement. The views and opinions expressed herein do not necessarily reflect the views of the European Commission.

REFERENCES

- [1]. G. Braithwaite et al., Rev. Sci. Instrum., **60**, 2825 (1989)
- [2]. G. Saibene et al., Nuclear Fusion, **39**, 1133 (1999)
- [3]. Gill.R.D et al., Nuclear Fusion, **40**, 163 (2000)
- [4]. A. Boboc et al., Rev. Sci. Instrum., **77**, 10F324 (2006)
- [5]. F. Orsitto et al., 47th Annual Meeting of the Division of Plasma Physics, Polarimetric measurements of line-integrated electron density at JET based on Cotton-Mouton effect in presence of large Faraday rotation, APS (2005)
- [6]. C. Mazzotta et al., International Workshop on Burning Plasma Diagnostics, Models Comparison for JET Polarimeter Data, villa Monastero, Varenna, (2007)
- [7]. H. Soltwisch, Rev. Sci. Instrum., **57**, 1986 (1939)
- [8]. D. Clarke and J.F. Grainger, Polarized Light and Optical Measurement, (Oxford: Pergamon) (1971)
- [9]. S. E. Segre, Plasma Phys. Control. Fusion, **35**, 1261 (1993)
- [10]. Ch. Fuchs, H. J. Hartfuss, Rev. Sci. Instrum., **70**, 722 (1999)
- [11]. K. Guenther, Plasma Phys. Control. Fusion, **46**, 1423-1441 (2004)

- [12]. M. Brombin, 34st EPS Conference on Plasma Physics, The line-integrated plasma density from both interferometry and polarimetry at JET, (2007).
- [13]. Hutchinson, Principles of Plasma Diagnostics, (Cambridge: Cambridge University Press) (1987)
- [14]. A. J .H .Donné et al., Rev. Sci. Instrum., **70**, 726 (1999)
- [15]. M. Born and E. wolf, Principles of Optics, Pergamon Press, Oxford (1980)
- [16]. F. De Marco and S. E. Segre, Plasma Phys. Control. Fusion, **14**, 245, (1972)
- [17]. S. E. Segre, Plasma Phys. Control. Fusion, **41**, R57-R100 (1999)
- [18]. K. Guenther, 31st EPS Conference on Plasma Physics, **P5**, 172 (London 2004)
- [19]. A. Murari et al., Rev. Sci. Instrum., **77**, 073505 (2006)

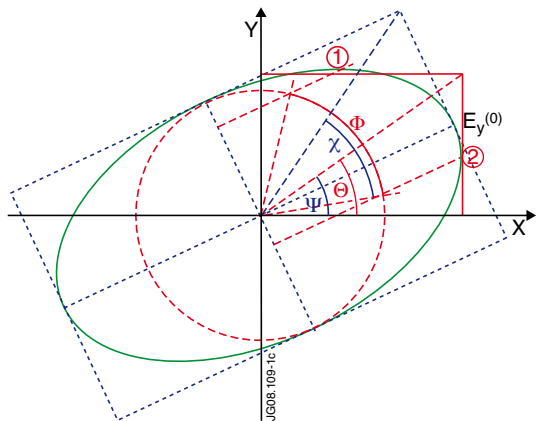


Figure 1: The polarization ellipse, with geometric (ψ , χ) and electric parameters (Θ , Φ)

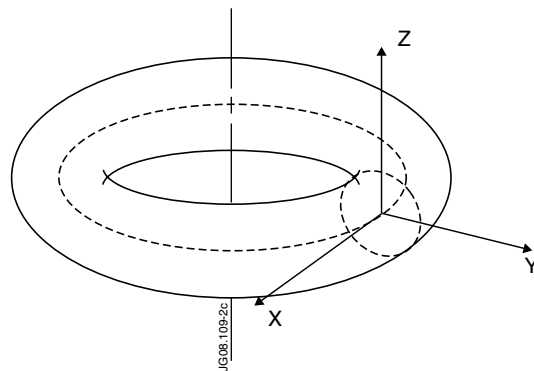


Figure 2: Reference system for a torus. The radiation is assumed to propagate along the z axis.

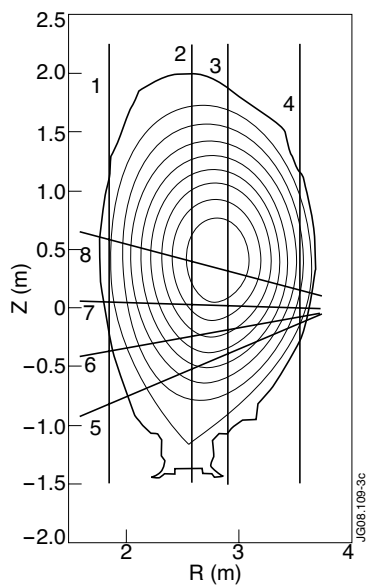


Figure 3: Lines of sight for interferometry and polarimetry at JET

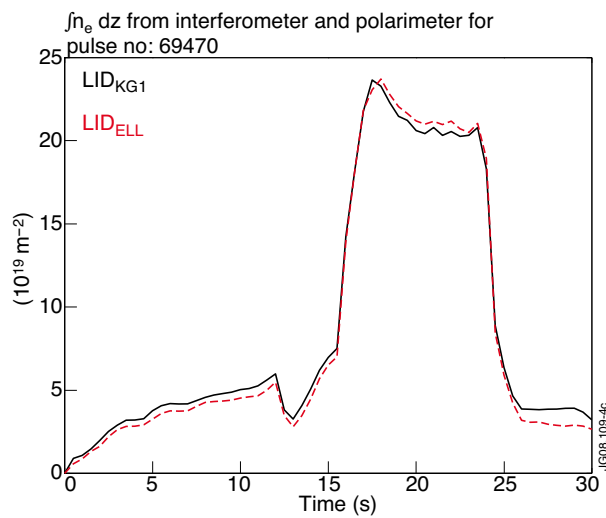


Figure 4: Comparison between the line integrated density evaluated by the interferometer (black line) and the polarimeter (red line)

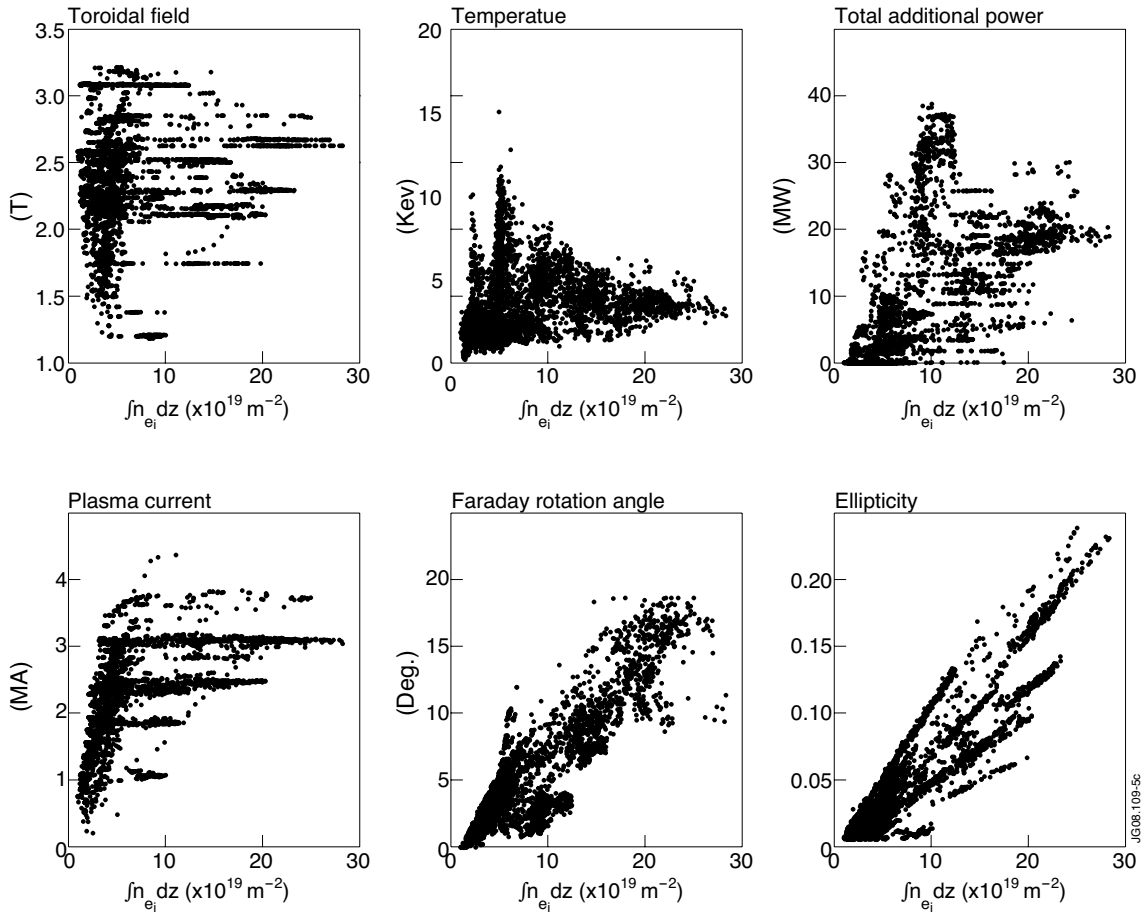


Figure 5: Statistical representation of the plasma parameters for all the considered shots as a function of the interferometric line integrated electron density.

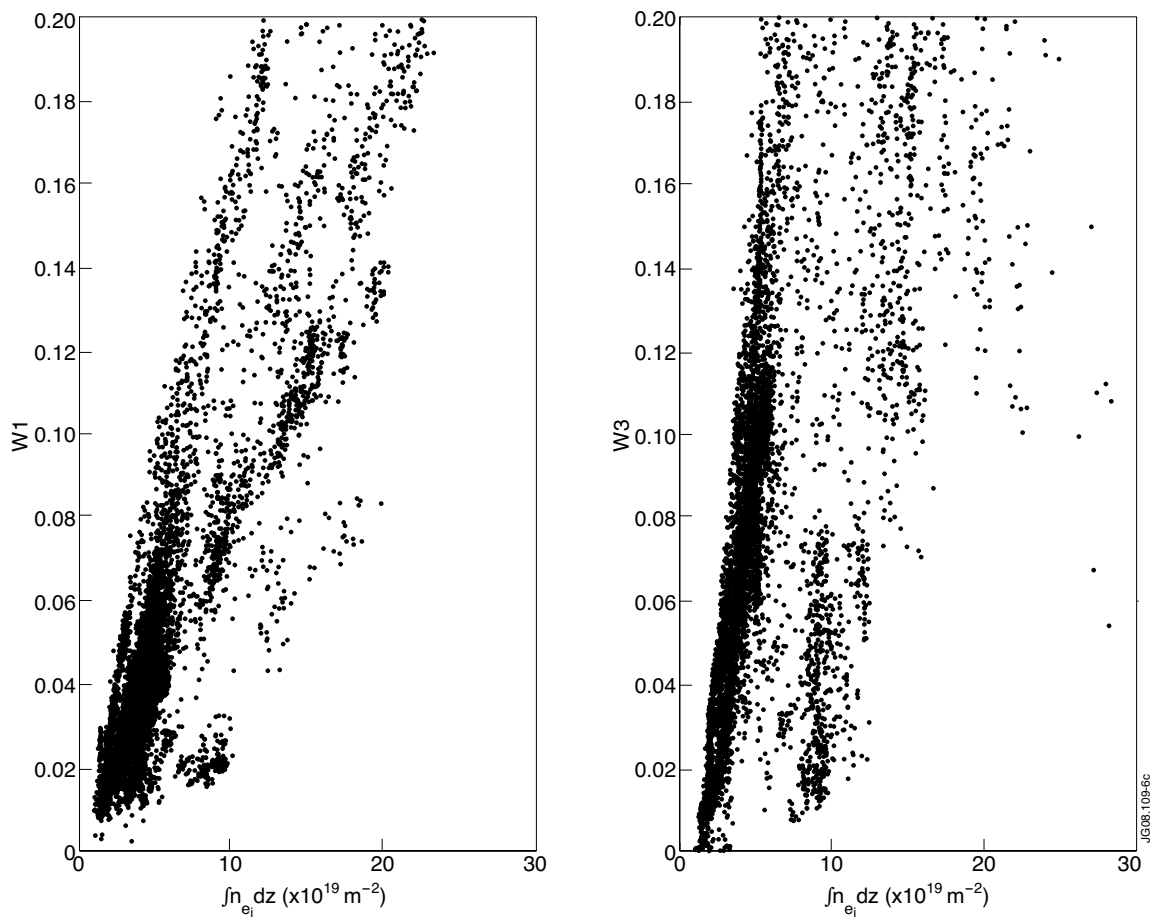


Figure 6: The polarization ellipse, with geometric (ψ , χ) and electric parameters (Θ , Φ)

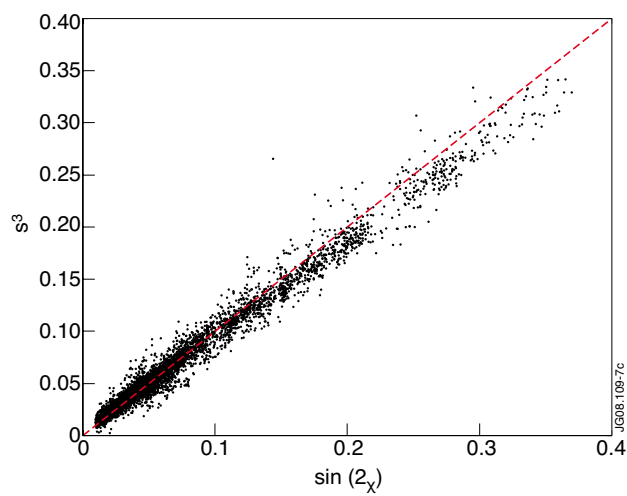


Figure 7: Behaviour of the W_1 and W_3 parameters for the entire density range.

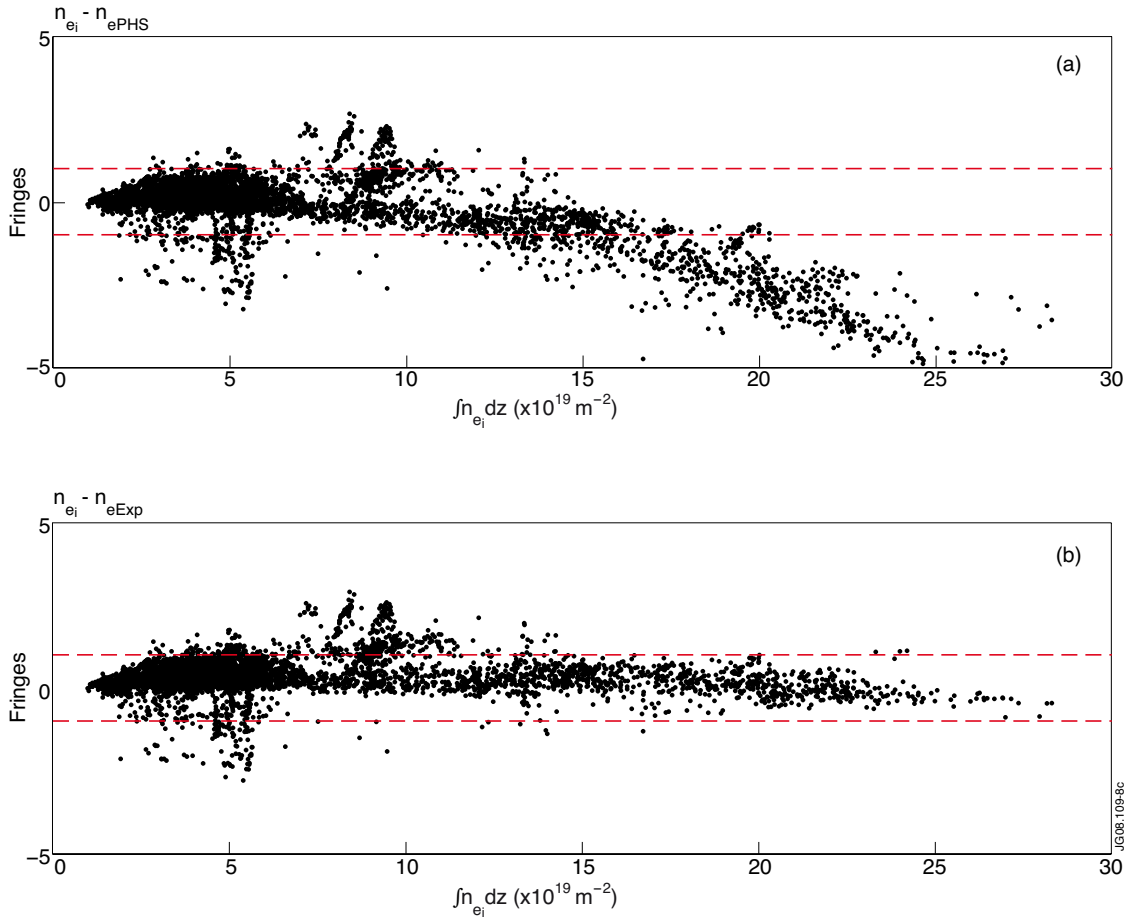


Figure 8: Difference between the line integrated density from polarimetric data and the interferometer line density in terms of fringes (one fringe = $1.143 \times 10^{19} \text{ m}^{-2}$). The density from polarimetry has been evaluated using equation (23) in a and equation (21) in b. The dotted red lines are the threshold reference of one fringe.

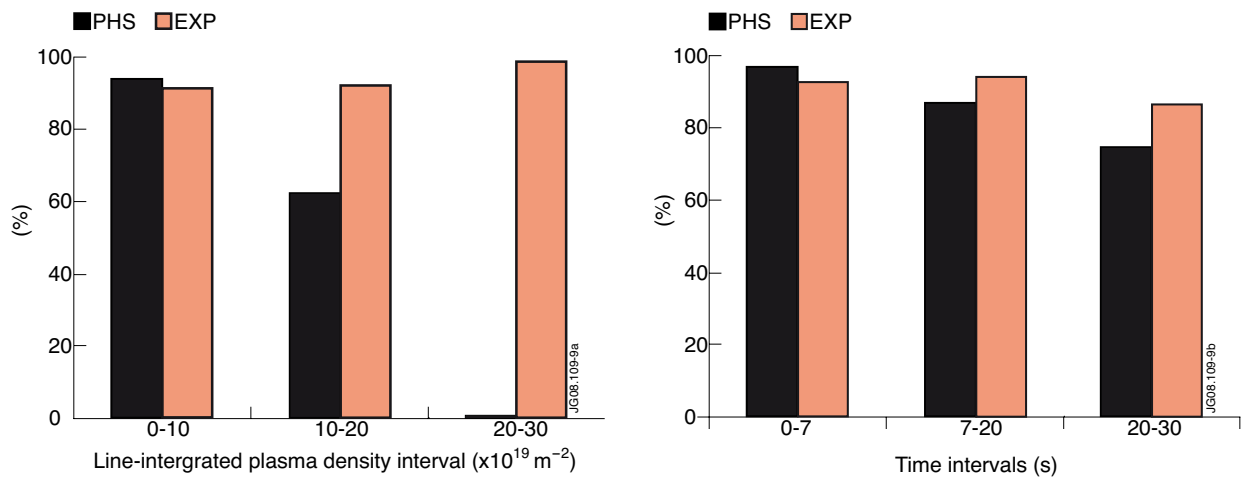


Figure 9: The bars in the histograms represent the fraction of points (in percents) for which the difference between density from polarimetry and from interferometry is within a fringe ($1.143 \times 10^{19} \text{ m}^{-2}$) over three different density and time ranges.

